Generalized One-Dimensional, Steady, Compressible Flow

Fred M. Young*
Lamar University, Beaumont, Texas 77710

Nomenclature

A = area
C = change coefficients
C_1 = coefficient given by Eq. (7)
C_2 = coefficient given by Eq. (8)
c_v = specific heat at constant volume
D = hydraulic diameter
F = generalized independent variable
f = friction coefficient
ff = function of parametric variables
f_n = Mach number functions from Shapiro[1]
g = static pressure mass flow function
k = specific heat ratio
L = length
M = Mach number
m = slope of hydraulic diameter vs x
P = isentropic stagnation pressure
p = static pressure
s = entropy
T = temperature
w = mass flow rate
x = distance in the direction of flow
y = injected flow velocity ratio

Subscripts

a = pertaining to area change
f = pertaining to fluid friction
max = length to the $M = 1$ state
s = pertaining to a singularity
t = pertaining to heat transfer
w = pertaining to mass flow injection
0 = isentropic stagnation state
1 = pertaining to section 1
2 = pertaining to section 2

Superscripts

$*$ = at $M = 1$
$'$ = nondimensionalized

Introduction

CLASSIC analysis of one-dimensional, steady, compressible flow of perfect gases is well documented; see, e.g., Refs. 1-4. The classic approach examines the simple case of each of the usual independent variables of compressible flow: area change, heat transfer, friction, and mass injection. Hodge[5] described the similarities of mass injection and the other simple changes. Each of these simple models involves a set of flow functions, usually tabulated as functions of Mach number.

Benedict and Stelz[6] present an extensive listing of simple-change flow functions both as a function of Mach number and other property ratios. In addition, they apply conservation of mass to certain two independent variable combined-change cases. The method basically involves multiplying their Γ function (numerically and conceptually the same as the stagnation pressure mass flow function divided by the same function evaluated at $M = 1$) by the appropriate property ratios. Their results can be replicated by applying simple changes sequentially with the nonisentropic change used first. Obviously, combined-change processes are path dependent. Therefore, such sequential application of simple changes cannot represent simultaneous changes of the independent variables.

Shapiro[1] also presents the traditional approach to combined-change problems, which begins with the constitutive differential equations, briefly addresses limited two independent variable cases and then quickly resorts to numerical procedures for the more general case. The combined-change problems present additional complexity as compared to simple changes since they depend on the path of the process. Beans[7] and Hodge[8] illustrate the numerical techniques in generalized computer programs for the solution of combined-change problems.

The analytic model described here assumes a relationship among the independent variables. This assumption specifies the process path and, thereby, limits the generality. The same constitutive equations used by these numerical techniques are then solved analytically. The differential equation for Mach number as a function of the usual independent variables of compressible flow taken from Shapiro[1] is given in the following:

$$\frac{\mathrm{d}M^2}{M^2} = f_1(M)\frac{\mathrm{d}A}{A} + f_2(M)\frac{\mathrm{d}T_0}{T_0} + f_3(M)\left(\frac{4f\mathrm{d}x}{D} - 2y\frac{\mathrm{d}w}{w}\right) + f_4(M)\frac{\mathrm{d}w}{w} \tag{1}$$

Where the $f_n(M)$ are given by the expressions

$$f_1(M) = -\left[\frac{2+(k-1)M^2}{1-M^2}\right]$$

$$f_2(M) = \left[\frac{(1+kM^2)\{1+[(k-1)M^2]/2\}}{1-M^2}\right]$$

$$f_3(M) = \left[\frac{kM^2\{1+[(k-1)M^2]/2\}}{1-M^2}\right]$$

$$f_4(M) = \left[\frac{2(1+kM^2)\{1+[(k-1)M^2]/2\}}{1-M^2}\right]$$

Generalized Model

The approach of the generalized model is to represent each of the independent variables by a constant change coefficient C and a generalized variable F, as shown in Eqs. (2-5):

$$\frac{\mathrm{d}A}{A} = C_a\frac{\mathrm{d}F}{F} \tag{2}$$

$$\frac{\mathrm{d}T_0}{T_0} = C_t\frac{\mathrm{d}F}{F} \tag{3}$$

$$\frac{4f\mathrm{d}x}{D} = C_f\frac{\mathrm{d}F}{F} \tag{4}$$

$$\frac{\mathrm{d}w}{w} = C_w\frac{\mathrm{d}F}{F} \tag{5}$$

The generalized variable will usually be identified as one of the formerly independent variables in a specific analysis. Substituting Eqs. (2-5) into Eq. (1) and integrating from $M = 1$ to M yields an expression for the generalized variable ratio, F/F^*:

$$F' = \left(\frac{F}{F^*}\right)^{C_1} = M^2 ff\left(M, k, \frac{C_2}{C_1}\right) \tag{6}$$

Received Dec. 2, 1991; revision received June 8, 1992; accepted for publication July 6, 1992.

*Professor of Mechanical Engineering and Dean, P.O. Box 10057.

Table 1 Generalized flow functions for $C_2/C_1 = 0$ and $k = 1.4$

M	F'	P_0'	p'	T'	s'
0.0000	0.0000	1.0000	1.8929	1.2000	0.0000
0.1000	0.0295	1.0000	1.8797	1.1976	0.0000
0.2000	0.1139	1.0000	1.8409	1.1905	0.0000
0.3000	0.2415	1.0000	1.7784	1.1788	0.0000
0.4000	0.3955	1.0000	1.6953	1.1628	0.0000
0.5000	0.5570	1.0000	1.5958	1.1429	0.0000
0.6000	0.7083	1.0000	1.4841	1.1194	0.0000
0.7000	0.8350	1.0000	1.3647	1.0929	0.0000
0.8000	0.9277	1.0000	1.2418	1.0638	0.0000
0.9000	0.9825	1.0000	1.1190	1.0327	0.0000
1.0000	1.0000	1.0000	1.0000	1.0000	0.0000
1.1000	0.9843	1.0000	0.8866	0.9662	0.0000
1.2000	0.9418	1.0000	0.7806	0.9317	0.0000
1.3000	0.8795	1.0000	0.6832	0.8969	0.0000
1.4000	0.8045	1.0000	0.5948	0.8621	0.0000
1.5000	0.7229	1.0000	0.5156	0.8276	0.0000
1.6000	0.6398	1.0000	0.4454	0.7937	0.0000
1.7000	0.5589	1.0000	0.3835	0.7605	0.0000
1.8000	0.4829	1.0000	0.3294	0.7282	0.0000
1.9000	0.4134	1.0000	0.2825	0.6969	0.0000
2.0000	0.3512	1.0000	0.2419	0.6667	0.0000

Table 2 Generalized flow functions for $C_2/C_1 = 0.5$ and $k = 1.4$

M	F'	P_0'	p'	T'	s'
0.0000	0.0000	1.1460	2.1694	1.2000	−0.0545
0.1000	0.0385	1.1421	2.1468	1.1976	−0.0531
0.2000	0.1456	1.1307	2.0815	1.1905	−0.0491
0.3000	0.2993	1.1134	1.9799	1.1788	−0.0430
0.4000	0.4717	1.0921	1.8515	1.1628	−0.0353
0.5000	0.6370	1.0694	1.7065	1.1429	−0.0268
0.6000	0.7770	1.0474	1.5543	1.1194	−0.0185
0.7000	0.8824	1.0280	1.4029	1.0929	−0.0111
0.8000	0.9519	1.0130	1.2579	1.0638	−0.0052
0.9000	0.9891	1.0033	1.1230	1.0327	−0.0013
1.0000	1.0000	1.0000	1.0000	1.0000	−0.0000
1.1000	0.9912	1.0035	0.8897	0.9662	−0.0014
1.2000	0.9688	1.0143	0.7917	0.9317	−0.0057
1.3000	0.9378	1.0326	0.7054	0.8969	−0.0128
1.4000	0.9018	1.0587	0.6298	0.8621	−0.0228
1.5000	0.8636	1.0930	0.5636	0.8276	−0.0356
1.6000	0.8252	1.1357	0.5058	0.7937	−0.0509
1.7000	0.7877	1.1872	0.4553	0.7605	−0.0686
1.8000	0.7519	1.2478	0.4111	0.7282	−0.0886
1.9000	0.7183	1.3181	0.3724	0.6969	−0.1105
2.0000	0.6870	1.3987	0.3384	0.6667	−0.1342

where

$$ff\left(M, k, \frac{C_2}{C_1}\right) = \left(\left\{\frac{(k+1)}{[2+(k-1)M^2]}\right\}^{(k+1)} \times \left\{\frac{[1+kM^2(C_2/C_1)]}{[1+k(C_2/C_1)]}\right\}^{2[1+k(C_2/C_1)]}\right)^{\frac{1}{k-1-2k(C_2/C_1)}}$$

$$C_1 = 2C_w + C_t - 2C_a \tag{7}$$

$$C_2 = C_t + C_f + 2C_w(1-y) \tag{8}$$

The function of the generalized variable on the left side of Eq. (6) is a function of Mach number M, specific heat ratio k, and change coefficient ratio C_2/C_1. Other properties may be obtained as functions of the same three variables. The expression for nondimensional temperature is derived in a straightforward manner from the relationship between the static and stagnation temperatures:

$$T' = \frac{T/T^*}{T_0/T_0^*} = \frac{(k+1)}{[2+(k-1)M^2]} \tag{9}$$

Expressions for the nondimensional static and stagnation pressures are found from the corresponding mass flow functions. Derivation is shown for only the static pressure beginning with the static pressure mass flow function:

$$\frac{w\sqrt{T_0}}{pA} = g(M, k), \qquad \frac{w^*\sqrt{T_0^*}}{p^*A^*} = g(1, k)$$

$$\frac{w\sqrt{T_0}}{pA}\frac{p}{p^*}\frac{A}{A^*}\sqrt{\frac{T_0^*}{T_0}}\frac{w^*}{w} = \frac{w^*\sqrt{T_0^*}}{p^*A^*} = g(1, k)$$

$$\frac{w\sqrt{T_0}}{pA}\frac{p}{p^*}\left(\frac{F}{F^*}\right)^{C_a}\left(\frac{F}{F^*}\right)^{\frac{-C_t}{2}}\left(\frac{F}{F^*}\right)^{-C_w} = g(1, k)$$

$$\frac{w\sqrt{T_0}}{pA}\frac{p}{p^*}\left(\frac{F}{F^*}\right)^{C_a - \frac{C_t}{2} - C_w} = g(1, k)$$

The unusual form of Eq. (6) now becomes a distinct advantage since the exponent of F/F^* is $-C_1/2$.

$$g(M, k)\frac{p}{p^*}\left(\frac{F}{F^*}\right)^{\frac{-C_1}{2}} = g(1, k)$$

$$\frac{p}{p^*} = \frac{g(1, k)M\sqrt{ff[M, k, (C_2/C_1)]}}{g(M, k)}$$

The right-hand side of this equation can be reduced to

$$p' = \frac{p}{p^*} = \sqrt{\frac{(k+1)}{[2+(k-1)M^2]}ff\left(M, k, \frac{C_2}{C_1}\right)} \tag{10}$$

The stagnation pressure is found in a similar manner utilizing the stagnation pressure mass flow function:

$$P_0' = \frac{P_0}{P_0^*} = \sqrt{ff\left(M, k, \frac{C_2}{C_1}\right)}\left\{\frac{(k+1)}{[2+(k-1)M^2]}\right\}^{[-(k-1)/(k+1)]} \tag{11}$$

All other properties may be derived in terms of those given in Eqs. (6) and (9–11). Entropy is derived in this manner and is shown in the following:

$$s' = \frac{(s-s^*)}{c_v} - kC_t \ln\frac{F}{F^*}$$
$$= \ln\left\{\sqrt{\frac{(k+1)^{(k+1)}}{[2+(k-1)M^2]^{(k+1)}ff[M, k, (C_2/C_1)]^{(k-1)}}}\right\} \tag{12}$$

On request, the author will provide a complimentary copy of PC-based software which calculates the generalized functions and their inverses.

Simple Changes

Application of the generalized model for the well-known cases of simple changes can serve to test both the model's validity and utility, as well as to demonstrate the details of model utilization. In all cases, the specific heat ratio of the gas will be taken as $k = 1.4$.

Area Change—Isentropic Flow

For simple area change, all other independent variables remain constant or zero in the case of friction. Therefore, the change coefficients of Eqs. (2–5) are all zero except for the area change coefficient C_a, which is taken as unity. This identifies the generalized independent variable F as the area A. The values of C_1 and C_2 from Eqs. (7) and (8) are -2 and 0, respectively. Refer to Table 1 for the applicable set of generalized flow functions calculated for $C_2/C_1 = 0$. The value of F' taken from the table is then interpreted as

$$F' = \left(\frac{A}{A^*}\right)^{-2}$$

The values of A/A^* are clearly correct at Mach numbers of 0 and 1. The value of A/A^* at $M = 2$ is calculated as

$$\frac{A}{A^*} = \frac{1}{\sqrt{0.3512}} = 1.6874$$

which is correct within the number of significant figures used. The constant value of P_0 and the zero value of $(s - s^*)$ are also correct for isentropic flow. The values of p/P_0 and T/T_0 are calculated for $M = 0.5$ as shown in the following:

$$\frac{p}{P_0} = \frac{p'(M)}{p'(0)} = \frac{1.5958}{1.8929} = 0.8430$$

$$\frac{T}{T_0} = \frac{T'(M)}{T'(0)} = \frac{1.1429}{1.2} = 0.9524 \quad \text{since} \quad \frac{T_0}{T_0^*} = 1$$

These values are correct within the number of significant figures used.

Note that this set of flow functions is applicable to a much broader range of processes than the simple area change process. These functions apply anytime C_2 is equal to zero. For example, for simple mass injection with $y = 1$, the functions apply with the generalized variable F identified as the mass flow rate w. In this case, $C_1 = 2$, and so w/w^* is the square root of F'. The property values for mass injection are consistent with those given by Hodge and Young.[9]

The last two columns of Table 1 are tabulations of the T' and s' values that describe loci of states on a $T' - s'$ diagram of the processes represented by the value of C_2/C_1. Figure 1 is a plot of these loci for a number of positive values of the ratio C_2/C_1 and for $C_1 = 0$. Three of these loci are labeled generalized Fanno, Rayleigh, and isentropic flow since they are applicable to these simple changes. These loci are generalized since they individually represent an infinite number of combined-change processes.

Simple T_0 Change

For simple T_0 change, the change coefficients are zero except for C_t, which is 1. The values of C_1 and C_2 from Eqs. (7) and (8) are then calculated to be 1. Equation (6) can easily be shown to be identical to T_0/T_0^* for this case. Properties from Eqs. (9–12) can similarly be shown to be consistent with those from a Rayleigh flow function table. The $C_2/C_1 = 1$ plot on the $T' - s'$ diagram of Fig. 1 is a generalized Rayleigh line. In fact, this same locus also represents simple injection with $y = 0$ (Ref. 5).

Simple Friction

Since the friction change coefficient does not appear in C_1 and all other coefficients are zero, the value of C_1 must be zero. The method of algebraically arranging Eqs. (6) and (9–12) causes their values to become indeterminate for $C_1 = 0$. When friction occurs in combination with other changes such that $C_1 \neq 0$, Eqs. (6) and (9–12) apply.

The flow functions for the special case of $C_1 = 0$ are included in the following for completeness. In this case, the system of equations are algebraically arranged with C_1 in the numerator of the constant ratio C_1/C_2, which is zero for this case. The generalized independent variable ratio and the same properties as given previously are listed in Eqs. (13–17).

$$F' = \left(\frac{F}{F^*}\right)^{C_2} = \left(\frac{2\{1 + [(k-1)/2]M^2\}}{(k+1)M^2}\right)^{[(k+1)/2k]} \exp \frac{-(1-M^2)}{kM^2} \tag{13}$$

$$p' = \frac{p}{p^*} = \sqrt{\frac{k+1}{2M^2\{1 + [(k-1)/2]M^2\}}} \tag{14}$$

$$P_0' = \frac{P_0}{P_0^*} = \frac{1}{M}\sqrt{\left\{\frac{[2 + (k-1)M^2]}{(k+1)}\right\}^{[(k+1)/(k-1)]}} \tag{15}$$

$$T' = \frac{T/T^*}{T_0/T_0^*} = \frac{k+1}{[2 + (k-1)M^2]} \tag{16}$$

$$s' = \frac{(s - s^*)}{c_v} - kC_t \ln \frac{F}{F^*} = \ln\left(M^{(k-1)}\sqrt{\left\{\frac{k+1}{[2 + (k-1)M^2]}\right\}^{k+1}}\right) \tag{17}$$

Equations (14–17) are identical to those for simple friction; however, they apply to all cases for which $C_1 = 0$. Equation (13) is very similar to that for $4fL_{max}/D$ derived for simple friction only rearranged to accommodate the functional relationship of the generalized variable. This functional relationship causes the mechanics of analyzing simple friction cases to change. For example, for air flowing in a duct of $4fL/D = 1.054567$ with an initial Mach number of 0.5. The Mach number at the end of the duct is found as shown in the following. Equation (13) is used at $M = 0.5$ to find

$$\left(\frac{F_1}{F^*}\right)^{C_2} = 0.343331$$

The ratio at section 2 is found as follows:

$$\left(\frac{F_2}{F^*}\right)^{C_2} = \left(\frac{F_1}{F^*}\right)^{C_2}\left(\frac{F_2}{F_1}\right)^{C_2} = 0.343331e^{1.054567} = 0.98561$$

The Mach number is then found from Eq. (13) as $M = 0.9$, which duplicates the result from simple friction tables for the same case.

Combined Changes

The primary advantage of this generalized model is the ability to approach combined-change problems analytically. Figure 1 indicates that the behavior of combined-change cases (for positive C_2/C_1) is very similar to that of the simple cases. Beginning at $M = 0$, the entropy increases as the Mach number increases until a point of maximum entropy is reached at $M = 1$. The value of the generalized independent, variable F' also increases with Mach number up to $M = 1$ and reaches a maximum at this point. As the Mach number increases above $M = 1$, the entropy and the generalized variable F' decrease. Just as is the case for simple changes, increasing F' above the value corresponding to $M = 1$ changes the upstream flow pattern. Static pressure decreases with increasing Mach number. Stagnation pressure decreases as the flow moves toward $M = 1$ from both subsonic and supersonic initial states. Temperature generally decreases with increasing Mach number. The cases that involve a more rapid increase in T_0/T_0^* than the decrease in T' are exceptions that are not obvious. These exceptions are most likely to occur in the subsonic regime as in the case of Rayleigh flow.

Analysis of a combined-change case is carried out in a manner similar to simple changes. The ratio F_2'/F_1' is used to relate the flow states at the beginning section 1 and the final section 2. Just as with simple changes, F^* is constant for flow along a locus of specified C_2/C_1 (see Fig. 1). As an example, take the case of air flowing at $M = 0.4$ at section 1. The ratios of the independent variables between sections 1 and 2 are specified for this example as

$$\frac{A_2}{A_1} = 1.2, \quad \frac{T_{02}}{T_{01}} = 1.2, \quad \frac{4fL}{D_1} = 0.095445, \quad \frac{w_2}{w_1} = 1.44 \quad \text{with } y = 1$$

Identifying the generalized variable as area (this is an arbitrary but useful selection), the change coefficients are then found from Eqs. (2–5) and the given data as $C_a = 1$,

$$C_t = \frac{\ln 1.2}{\ln 1.2} = 1, \qquad C_w = \frac{\ln 1.44}{\ln 1.2} = 2$$

and $C_f = 0.5$. The modeling for C_f should be developed in a bit more detail. Assuming the hydraulic diameter squared is proportional to the area (circles and squares for example) then

$$\frac{dA}{A} = 2\frac{dD}{D}$$

Further assuming that the diameter is a linear function of distance ($D = mx + b$) then

$$\frac{4f\,dx}{D} = \frac{2f}{m}(2)\frac{d\,mx}{mx+b} = \frac{2f}{m}(2)\frac{dD}{D} = \frac{2f}{m}\frac{dA}{A}$$

which gives,

$$C_f = \frac{2f}{m} = \frac{2f}{(D_2 - D_1)/L} = \frac{2fL}{D_1[(D_2/D_1) - 1]} = \frac{2fL}{D_1[\sqrt{(A_2/A_1)} - 1]}$$

The value of C_f is then 0.095445/2/(1.095445-1) = 0.5. The values of C_1 and C_2 are, respectively, 3 and 1.5, which results in a ratio C_2/C_1 of 0.5. Generalized functions calculated for this case are shown in Table 2. The value of the generalized variable, previously chosen to be the area, at section 2 may be found as

$$F_2' = F_1'\left(\frac{F_2}{F_1}\right)^3 = F_1'\left(\frac{A_2}{A_1}\right)^3 = 0.4717(1.2)^3 = 0.8151$$

A linear interpolation of Table 2 gives a Mach number of 0.636. Since a test of the generalized model is part of the objective, the functions are calculated more accurately from Eqs. (6) and (9–11) as

$$M_2 = 0.6324, \qquad F_2' = 0.8151, \qquad p_2' = 1.5049$$

$$T_2' = 1.1111, \qquad P_{02}' = 1.0407$$

The property ratios between sections 1 and 2 are

$$\frac{P_{02}}{P_{01}} = \frac{1.0407}{1.0921} = 0.9529, \qquad \frac{p_2}{p_1} = \frac{1.5048}{1.8515} = 0.8128$$

$$\frac{T_2}{T_1} = \frac{1.1111(1.2)}{1.1628} = 1.1466$$

For the purpose of comparison, an influence coefficient method is used to numerically integrate the constitutive equations for the same problem. The results of the integration are compared with the analytic method in the following:

Parameter	Numerical integration	Generalized method
M_2	0.6323	0.6324
P_{02}/P_{01}	0.9530	0.9529
p_2/p_1	0.8129	0.8128
T_2/T_1	1.1467	1.1466

The results agree within the estimated error for the numerical solution. A primary advantage for an analytic model is the ability to establish flow limitations without resorting to an iterative solution. For example, in this analysis, a limiting value of the generalized variable is $F' = 1$. Therefore, the maximum values of the parameters (assuming increases consistent, with constant, values of the change coefficients C_1 and C_2) would be

$$M_3 = 1, \qquad \frac{A_3}{A_1} = 1.285, \qquad \frac{T_{03}}{T_{01}} = 1.285$$

$$\frac{4fL}{D_1} = 0.1336, \qquad \frac{w_3}{w_1} = 1.650$$

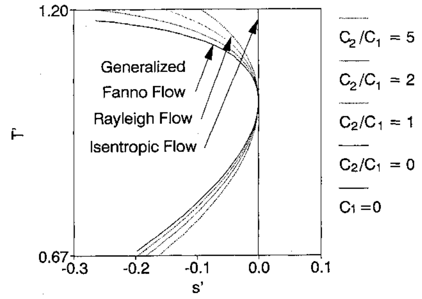

Fig. 1 Generalized $T' - s'$ diagram for $k = 1.4$.

Normal Shocks in Combined-Change Processes

Since normal shocks occur within a very short distance in the direction of flow, sequential modeling of the overall process as a combined-change process, followed by a normal shock, followed by the remainder of the combined-change process gives accurate results without compromising generality. Viewing such processes in terms of Fig. 1 the normal shock occurs from a point below the maximum entropy point to a point above the maximum entropy point (from supersonic to subsonic) on the same C_2/C_1 locus. The second point must always be to the right of the first point since entropy increases across a normal shock. When viewing the process on Fig. 1, it would be easy to draw the erroneous conclusion that the $M = 1$ state for the C_2/C_1 locus was the same before and after the shock. This conclusion is, true only for the case of $C_2/C_1 = 1$, which includes Rayleigh and injection type ($y = 0$) flows as well as other combined-change flows. For the latter cases, Eqs. (7) and (8) give the following relationship for the change coefficients.

$$C_f - 2C_w y + 2C_a = 0$$

For $C_2/C_1 \neq 1$, the $M = 1$ state changes and, therefore, the loci on a dimensional Mollier diagram are different for the combined-change process upstream of the shock and the process downstream of the shock.

Model Limitations

The change coefficient concept basically requires that the relative rate of change of all of the independent variables be related as a power function of the ratios. This variation might be recognized as that often assumed in numerically analyzing combined-change problems so that the log of the property ratio remains constant between step intervals. In many cases, this is a desirable feature. The single process path represented by the assumed relation among these variables limits the generality of the method. When substantial differences in the relative rates of change are needed, one way to work around this limitation is to break the problem into a number of sequential problems that can approximate the desired variation. Whereas the resulting numerical method can offer calculational efficiencies in some cases, the benefits would need to be substantial to justify replacing more accepted numerical methods.

Conclusions

A generalized method for analytically examining one-dimensional steady flow of perfect gases is proposed, developed, and tested. Area change, heat transfer, friction, and mass injection are allowed. Assuming that all independent variables depend on the same function allows the analytic solution while limiting the generality of the method. Generalized flow functions are developed and example tables are calculated. The tabular data are tested for both the simple cases and combined changes. A generalized $T' - s'$ diagram with a family of loci, each corresponding to a value of C_2/C_1, is shown to describe simple changes as well as combined changes. Normal shocks are shown to occur from the supersonic portion of these loci to the subsonic portion in a manner analogous to simple-change behavior. Normal shocks change the $M = 1$ state for all values of C_2/C_1 except $C_2/C_1 = 1$. This state change in turn affects the maximum change the flow can sustain without changing the initial flow conditions.

References

[1]Shapiro, A. H., *The Dynamics and Thermodynamics of Compressible Fluid Flow,* Vol. 1, Wiley, New York, 1953.

[2]Chapman, A. J., and Walker, W. F., *Introductory Gas Dynamics,* Holt, Rinehart and Winston, New York, 1971.

[3]Zucrow, M. J., and Hoffman, J. D., *Gas Dynamics,* Wiley, New York, 1976.

[4]Saad, M. A., *Compressible Fluid Flow,* Prentice-Hall, Englewood Cliffs, NJ, 1985.

[5]Hodge, B. K., "Process Path for Simple Mass Addition in One-Dimensional Compressible Flow," *International Journal of Applied Engineering Education,* Vol. 7, No. 1, 1991, pp. 51–55.

[6]Benedict, R. P., and Stelz, W. G., *Handbook of Generalized Gas Dynamics,* Plenum, New York, 1966.

[7]Beans, E. W., "Computer Solutions to Generalized One-Dimensional Flows," *Journal of Spacecraft and Rockets,* Vol. 7, No. 12, 1970, p. 1460.

[8]Hodge, B. K., "Generalized One-Dimensional Compressible Flow Techniques," *International Journal of Applied Engineering Education,* Vol. 7, No. 1, 1991, pp. 56–63.

[9]Hodge, B. K., and Young, F. M., "Simple Mass Addition Processes in One-Dimensional Compressible Flow," AIAA Paper 93-0487, Jan. 1993.

Subharmonic and Harmonic Forced Response of the Wake of a Circular Cylinder

Mohammad Javed Khan* and Anwar Ahmed†
Texas A & M University,
College Station, Texas 77843

Nomenclature

A = amplitude of splitter plate oscillation normalized by cylinder diameter
Cd_{norm} = drag of cylinder with splitter plate normalized by drag of cylinder without splitter plate
d = diameter of the cylinder
F = frequency of oscillation of splitter plate
f = von Kármán shedding frequency
S = Strouhal number, fd/U_o
S_f = forced Strouhal number, Fd/U_o
U_o = freestream velocity

Introduction

CAPABILITY to control frequency of vortex shedding from bluff bodies has applications ranging from wind engineering to altering of acoustic signatures of submerged vessels. Similarly, drag reduction of such bodies has always been a great concern of design engineers. A major effort in research on bluff body wakes has therefore been directed toward two aspects, namely, control of the shedding frequency and increase in base pressure. An excellent discussion of the various passive techniques to control vortex shedding can be found in a review paper by Zdravkovich.[1] Various mechanisms like base bleed, base cavity, and v grooves for increasing base pressures have also been explored by researchers.[2] Attention has also been directed toward active control of the wake width and vortex shedding frequency[3] by influencing the wake by either transverse vibrations or rotational oscillations of the cylinder or by acoustic energy input in the wake.

Monkewitz et al.[4] more recently used a linearized version of the complex Ginzburg-Landau equation to predict the global mode instability and used transverse vibrations of the cylinder as the actuator in a constant gain feedback control system to modify the wake. Their study, which was limited to S/S_f of 1.089 due to the cylinder material, concluded the ineffectiveness of the method beyond a Reynolds number of 90. However, by using an acoustic source as the actuator in a feedback control system, Ffowcs and Zhao[5] had shown that wake modification was possible at higher Reynolds numbers ($\sim 12 \times 10^3$).

The present research was motivated by the need to evaluate other practical wake modification devices having a potential of being placed in a closed-loop control system for controlling the wake. In this experimental investigation, an oscillating splitter plate located at the attachment line of a two-dimensional circular cylinder was tested as a candidate active of a feedback control system. Pertinent results of this investigation are presented.

Experimental Setup

The experiments were performed in the 0.5×0.9 m (2×3 ft) water tunnel and 0.45×0.45 m (18×18 in.) wind tunnel at the Texas A & M University. Plexiglass cylinders mounted between end plates were used as test models. A splitter plate of width $0.25d$ was pivoted between the end plates and oscillated about its trailing edge by a B & K shaker through a rigid tie-rod mechanism. A flexible seal was used to isolate the upper and lower surfaces near the attachment line of the cylinder.

The test conditions of a wind-tunnel speed of 15 m/s and water tunnel speed of 15 cm/s resulted in subcritical Reynolds numbers (based on cylinder diameter) of 3.1×10^4 and 1.4×10^4, respectively. Shedding frequency for the wind-tunnel model was estimated to be 98 Hz and for the water tunnel model to be 0.5 Hz using a Strouhal number (S) of 0.2. It was therefore decided to evaluate the subharmonic response of the wake in the wind tunnel and the higher harmonic response in the water tunnel because of limitations on the shaker.

The wake power spectra and shedding frequency were monitored using a hot-film sensor in the wake for use in the feedback loop, although for more practical applications a surface mounted sensor is envisaged (Fig. 1). For this investi-

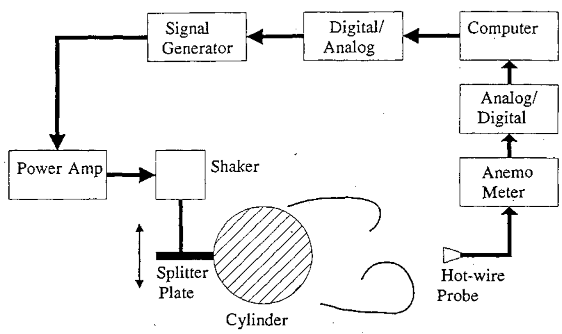

Fig. 1 Schematic of feedback control system.

Received Sept. 24, 1991; revision received June 20, 1992; accepted for publication July 7, 1992.

*Graduate Student, Aerospace Engineering Department.

†Assistant Professor, Aerospace Engineering Department. Member AIAA.